# Supplementary Appendix

# Raison d'être of insulin resistance: the adjustable threshold hypothesis

**Guanyu Wang**

**wang.gy@sustc.edu.cn**

## Mathematical modeling of glucose-insulin homeostasis

In the fasting state, plasma glucose is primarily utilized by the brain, which relies absolutely on glucose as its fuel. The glucose consumption is balanced by hepatic glucose production, which allows the body to maintain a relatively constant glucose concentration 65–105 mg/dl. Insulin also maintains a relatively constant concentration 5–10 $\mu$U/ml. In the mathematical modeling, $G_0 = 95$ mg/dl and $I_0 = 8$ $\mu$U/ml are used to be the fasting glucose and insulin concentrations.

Upon a meal ingestion, the plasma glucose concentration rises dramatically, intensifying its stimulation to the pancreas. Accordingly, the pancreas secretes more insulin and causes a surge of the plasma insulin concentration. The increased insulin concentration drains glucose from the blood into individual cells, which cancels out the initial surge of plasma glucose. The decrease of the glucose concentration is followed by the decrease of the insulin concentration, because the pancreas becomes less stimulated. Finally, both glucose and insulin return to their baseline levels.

Cells can be roughly divided into two categories according to their dependence on insulin for glucose uptake. The first category includes neurons whose glucose utilization is insulin independent. They uptake glucose continuously with a relatively constant rate, which is a factor contributing to the reduction of plasma glucose and insulin concentrations. The second category includes myocytes and adipocytes whose glucose utilization depends on insulin.

Because the increase of insulin is caused by the increase of glucose, but the increase of insulin causes the decrease of glucose and the consequential decrease of insulin, the system is essentially a

negative feedback one. It is this negative feedback that tightly regulates whole-body glucose-insulin homeostasis, namely the maintenance of the relative constancy of both concentrations even under the frequent perturbations from meal ingestion.

In [App1, App2], a mathematical model was developed for the glucose-insulin homeostatic system:

$$\begin{aligned}\frac{dG(t)}{dt} &= s + m(t) - V\big(I(t)\big)G(t),\\ \frac{dI(t)}{dt} &= f\big(G(t)\big) - kI(t),\end{aligned}$$

where

$t$ is the time.

$G(t)$ is the glucose concentration in the blood.

$I(t)$ is the insulin concentration in the blood.

$s$ is the glucose source rate supplied by the liver.

$m(t)$ is the rate of glucose supplied by a meal; one has $m(t) \equiv 0$ during fasting.

$k$ is the degradation rate of insulin.

$f(G)$ is the rate of insulin production by pancreatic beta cells in response to glucose stimulation; It is a monotonically increasing function of the glucose concentration [App1].

$V\big(I\big)$ is the body's rate of glucose uptake per unit glucose concentration.

The rate $V\big(I\big)$ marks the major difference among different models. In [App1], $V\big(I\big)$ was assumed to be a linear function of $I$. In [App2], $V\big(I\big)$ was initially undefined; but was found to be bistable should the system have certain optimal properties. In this paper, $V\big(I\big)$ is based on the insulin clamp data published in [App3, App4], which have been presented in figure 3A in two different sets of units. For the rate $V$, both units $\mathrm{min}^{-1}$ and $\mathrm{mg{\cdot}min^{-1}{\cdot}m^{-2}}$ are used. The conversion between the two units is as follows:

$$V \cdot G_0 = \frac{\tilde{V} \cdot S}{\Omega}, \tag{S.1}$$

where $V$ and $\tilde{V}$ correspond to the unit $\text{min}^{-1}$ and $\text{mg}\cdot\text{min}^{-1}\cdot\text{m}^{-2}$, respectively; $G_0 = 95$ $\text{mg}\cdot\text{dl}^{-1}$ is the baseline glucose concentration in the body; $S = 1.77$ $\text{m}^2$ is the subject's body surface area [App3]; and $\Omega$ is the subject's blood volume. Because an average adult has 5 to 6 liters of blood volume, $\Omega = 5.5$ liters is used here. One thus has:

$$V = 0.00034 \cdot \tilde{V}. \tag{S.2}$$

Therefore, 100, 200, 300, 400 $\text{mg}\cdot\text{min}^{-1}\cdot\text{m}^{-2}$ correspond to 0.034, 0.068 0.102, 0.136 $\text{min}^{-1}$, respectively. For the insulin concentration $I$, both units $\log_{10}(\mu\text{U/ml})$ and $\mu\text{U/ml}$ are used.

Figure 3A contains three sets of data: green (for normal subjects), red (for obese non-diabetes), and black (for obese diabetes). For all the cases, $V(I)$ can be divided into two components

$$V(I) = V_0 + U(I), \tag{S.3}$$

where

$V_0 = 0.025$ $\text{min}^{-1}$, as the baseline in figure 3A, is the rate of *insulin independent* glucose uptake. It is also independent of the health state. For normal subjects, obese non-diabetes, and obese diabetes, $V_0$ is always around 0.025 $\text{min}^{-1}$. This basal glucose uptake is contributed primarily by the brain, which needs to actively take up glucose with no regard of the insulin concentration and the health status.

$U(I)$ is the rate of *insulin mediated* glucose uptake. It ranges from 0 to a maximal rate $U_{\max}$. For the normal subjects, $U_{\max} = V_{\max} - V_0 = 0.139 - 0.025 = 0.114$ $\text{min}^{-1}$. This maximal rate is non-physiological, however, because the corresponding insulin concentration is about 20000 $\mu$U/ml — a supramaximal value. Under normal conditions, the peak insulin concentration after a regular meal is about 50 $\mu$U/ml (figure 4B), at which the rate of insulin mediated glucose uptake is only half maximal (figure 3A). The two figures together may suggest that insulin has great potential in rendering glucose uptake; but the potential is far from being reached under normal conditions.

Table S.1 summarizes all the parameter values used in the mathematical model, including $V_0 = 0.025$ $\text{min}^{-1}$. These parameter values are based on published works (see the references in Table S.1) and are thus biologically relevant. Besides the parameter values, the function forms of

$m(t)$ and $f(G)$ are also presented in Table S.1.

In the main text, two fundamentally different hypotheses are proposed for single-cell insulin response, which lead to two different interpretations of $U(I)$ — the rate of insulin mediated glucose uptake.

Table S.1: Parameters and special functions in the model

| Parameter/function | Value | Unit | Remark |
|---|---|---|---|
| $G_0$ | 95 | $\mathrm{mg{\cdot}dl^{-1}}$ | Baseline glucose level should be in the range |
| | | | of 65–105 [App5] |
| $I_0$ | 8 | $\mu\mathrm{U{\cdot}ml^{-1}}$ | Baseline insulin level should be in the range |
| | | | of 5–10 [App6] |
| $V_0$ | 0.025 | $\mathrm{min^{-1}}$ | Basal (insulin independent) rate of glucose |
| | | | utilization [App3, App4] |
| $s$ | 2.375 | $\mathrm{mg{\cdot}dl^{-1}{\cdot}min^{-1}}$ | Determined by the relation $s/V_0 = G_0$ |
| $k$ | 0.3 | $\mathrm{min^{-1}}$ | [App7, App8] |
| $G_h$ | 141.4 | $\mathrm{mg{\cdot}dl^{-1}}$ | Obtained from $G_h = \alpha^{0.5}$ and $\alpha = 20000$ [App9, App1] |
| $n$ | 6 | | $n > 4$ is required to generate dynamics close to |
| | | | clinical data in [App10, App11] |
| $f_{\max}$ | 28.5 | $\mu\mathrm{U{\cdot}ml^{-1}{\cdot}min^{-1}}$ | Determined by the relation $f_{\max} = kI_0(1 + (G_h/G_0)^n)$ |
| $\tau_1$, $\tau_2$, $\tau_3$ | 15, 30, 100 | min | To mimic the glucose intake pattern in [App11] |
| $M$ | 12.0 | $\mathrm{mg{\cdot}dl^{-1}{\cdot}min^{-1}}$ | The peak rate of exogenous glucose supply. |
| | | | The choice renders the dynamics close to the data in [App10] |
| $f(G) = \frac{f_{\max}(G/G_h)^n}{1+(G/G_h)^n}$ | | $\mu\mathrm{U{\cdot}ml^{-1}{\cdot}min^{-1}}$ | Rate of insulin production by the pancreas |
| $m(t) = \frac{M(t/\tau_1)^b}{1+(t/\tau_1)^b}$ | | $\mathrm{mg{\cdot}dl^{-1}{\cdot}min^{-1}}$ | Rate of glucose supplied by meal for $0 \le t < \tau_2$ |
| $m(t) = \frac{M\cdot\exp(c(\tau_3-t))}{1+\exp(c(\tau_3-t))}$ | | $\mathrm{mg{\cdot}dl^{-1}{\cdot}min^{-1}}$ | Rate of glucose supplied by meal for $\tau_2 \le t < \infty$ |

## The graded response view

Figure S.1 is a schematic diagram of the graded response view, where four example cells are illustrated with their response curves placed to the left, which from top down are more and more sensitive to insulin. Despite their individuality, these response curves are all graded, qualitatively the same as each other and as the whole-body dose response, which is just simple accumulations of single-cell responses:

$$U(I) = \sum_k u_k(I), \tag{S.4}$$

where $k$ numbers the cells. The graded response view provides the simplest and most intuitive explanation of the graded whole-body dose-response. Indeed, if an individual response $u_k(I)$ is graded, then the whole-body response $U(I)$, according to equation S.4, is certainly graded.

Moreover, the whole-body dose-response $U(I)$ must exhibit exact reversal, i.e.,

$$U^+(I) = U^-(I), \tag{S.5}$$

where the superscript $+(-)$ signifies the increase (decrease) of insulin. Indeed, if individual cells exhibit the graded response, they must also exhibit exact reversal ($u_k^+(I) = u_k^-(I)$). One then has

$$U^+(I) = \sum_k u_k^+(I) = \sum_k u_k^-(I) = U^-(I), \tag{S.6}$$

namely an exact reversal of the whole-body response. In other words, if the whole-body response does not exhibit exact reversal, then the graded response view must be wrong. As I have explained in the main text, the exact reversal of the whole-body response is contradictory to a frequently observed phenomenon known as reactive hypoglycemia. This fact will be demonstrated by numerical simulations below.

Under the graded response view, the numerical computation is relatively easy, because $V(I)$ is exactly the green curve in figure 3A. By using this $V(I)$ and the parameter values in Table S.1, equations 1 and 2 are integrated to yield simulated glucose and insulin dynamics (figure 5). The

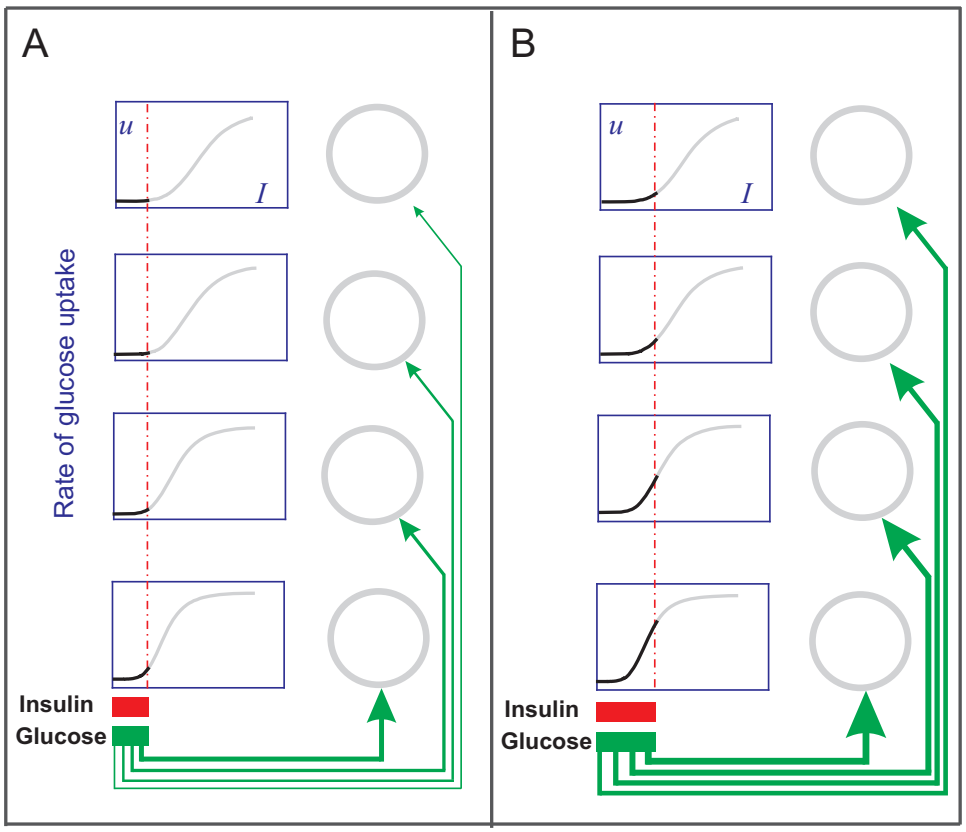


***Figure*** S.1: **The graded response view**. Under this view, a cell's rate of glucose uptake increases gradually as the insulin concentration increases. Four example cells are shown, which from top down are more and more sensitive to insulin. But the responses are all graded. The green and red bars represent the plasma glucose and insulin concentrations, respectively. (A) When the plasma insulin concentration is low, the cells absorb glucose with lower rates. (B) When the plasma insulin concentration is high, the cells absorb glucose with higher rates, indicated by the thicker green arrows.

simulation starts at $t = 0$ when the meal ingestion begins and ends at $t = T$ when homeostasis has been restored. In this paper $T = 1200$ min is used. Because the glucose level $G(t)$ is always above the baseline $G_0$, an undershoot does not occur during the simulation, let alone reactive hypoglycemia. In the following, I use the quantity $G(T)/G_0 - 1$ as an indicator of hypoglycemia. If the quantity is smaller than 0, then an undershoot occurs.

To see how representative this observation is, the simulation is repeated $10^4$ times, each with a new set of parameter values. For every round of simulation, the value of every parameter is drawn randomly from a uniform distribution centering on the standard value (i.e., the value in Table S.1) with $\pm 40\%$ variation. That is, every parameter value is generated with equal probability between $1 - 40\%$ and $1 + 40\%$ of its standard value. With this set of parameter values, equations 1 and 2

are solved numerically. The quantity $G(T)/G_0 - 1$ is then computed. For all the $10^4$ simulations, the quantity is always found to be positive, i.e., reactive hypoglycemia never occurs. Figure S.2A shows the histogram of these $10^4$ values of $G(T)/G_0 - 1$. One sees that the histogram is strictly to the right of the longitudinal axis.

Now, one sees the problem of the graded response view. Under this view, the whole-body dose-response $V\,(I)$ must be a simple curve that exhibits exact reversal. But this $V\,(I)$ is unable to even generate an undershoot of the glucose dynamics; and reactive hypoglycemia would certainly never occur because it corresponds to a large undershoot. Because reactive hypoglycemia is a frequently observed phenomenon, the graded response view may well be wrong, even though it is simple and intuitively appealing.

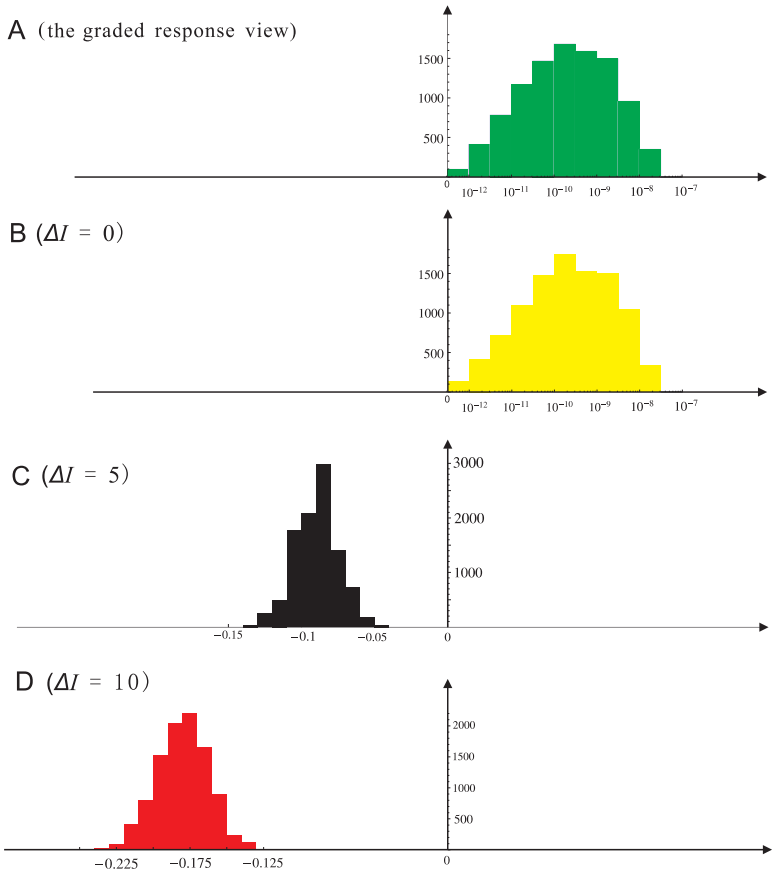


***Figure*** S.2: **Histograms of the quantity** $G(T)/G_0 - 1$. (A) is obtained under the graded response view. (B, C, D) are obtained under the adjustable threshold hypothesis with different levels of hysteresis.

## The adjustable threshold hypothesis

According to this hypothesis, a typical cell exhibits all-or-none and hysteretic reversal when responding to insulin (the third row of figure 6). The all-or-none property does not retain at the whole-body level, because cellular heterogeneity smoothes out individual all-or-none. In the second row of figure 6, cells with larger $I_{\text{on}}$ values are placed to the right of those with smaller $I_{\text{on}}$ values; and a Gaussian distribution is assumed. On the other hand, the whole-body response does inherit the property of hysteretic reversal. The same insulin concentration can elicit both a relatively low rate of glucose uptake ($V^+(I)$: the forward branch of $V(I)$) and a relatively high rate of glucose uptake ($V^-(I)$: the reverse branch of $V(I)$). As a consequence, insulin becomes more "powerful" during its fall — a rather counterintuitive conclusion. Nevertheless, it can explain reactive hypoglycemia, a recurring phenomenon that remains elusive. The reverse branch of $V(I)$ implies that glucose uptake can still be relatively high when the insulin level has been low. Due to the parallelism between insulin and glucose levels, this implies that glucose uptake can still be relative high when the glucose level has been low, which leads to hypoglycemia.

In this event, normal subjects' insulin clamp data (the green dots $(I_j, V_j)$ in figure 3A) only correspond to $V^+(I)$. According to the adjustable threshold hypothesis, $V_j$ is proportional to the number of cells activated by the rising insulin (i.e., those cells whose $I_{\text{on}}$ values are smaller than $I_j$). Therefore, if the cells' distribution is taken to be Gaussian with mean $\mu$ and standard deviation $\sigma$, then the dose-response curve is a cumulative Gaussian function

$$V^+(I) = V_0 + \frac{V_{\max} - V_0}{2}\left(1 + \operatorname{erf}\left(\frac{I-\mu}{\sqrt{2}\sigma}\right)\right), \tag{S.7}$$

where $V_0 = 0.025\ \text{min}^{-1}$. By using $\mu = 1.68$, $\sigma = 0.34$, $V_{\max} = 0.139\ \text{min}^{-1}$ in equation S.7, a curve $V^+(I)$ is generated that fits well with the green dots. The curve is colored in green in figure 3A. The corresponding Gaussian distribution ($\mu = 1.68$, $\sigma = 0.34$) is illustrated as the green curve in figure 3B.

I use numerical simulations to test the adjustable threshold hypothesis. Because the reverse branch $V^-(I)$ is not given, I take an agent-based approach, namely take individual cells into the

model. A system of $N = 10^5$ cells is first created *in silico*, with their $I_{\text{on}}$ values specified by the Gaussian distribution (1.68, 0.34) (the green curve in figure 3B). For each cell, a number $x$ is drawn from the Gaussian distribution (1.68, 0.34); and the value $10^x$ is assigned to the cell as its $I_{\text{on}}$ value in the unit $\mu$U/ml. For the $I_{\text{off}}$ values, I assume all the $N = 10^5$ cells have the same $\Delta I$ value. That is, if a cell's $I_{\text{on}}$ is $10^x$ for some $x$, then its $I_{\text{off}}$ is $10^x - \Delta I$.

In equations 1 and 2, one still has

$$V(I) = V_0 + \sum_k u_k(I), \tag{S.8}$$

the same as the last section. The difference lies in the fact that $u_k(I)$ is now bistable (see figure 2B). By omitting the subscript $k$, $u(I)$ has the following expression:

$$u\left(I\left(t\right)\right) = \begin{cases} 0 & 0 < I\left(t\right) \leq I_{\text{off}} \\ u\left(I\left(t^-\right)\right) & I_{\text{off}} < I\left(t\right) \leq I_{\text{on}} \\ u_{\max} & I\left(t\right) > I_{\text{on}} \end{cases}, \tag{S.9}$$

where $t$ is the present moment, $t^-$ is a time infinitesimally prior to $t$, $I_{\text{on}}$ represents the cell's switch-on threshold, $I_{\text{off}}$ represents the cell's switch-off threshold, $u_{\max}$ is the cell's maximal rate of glucose uptake. When the insulin concentration is smaller than $I_{\text{off}}$, the cell's glucose uptake rate is certainly 0. When the insulin concentration is larger than $I_{\text{on}}$, the cell's glucose uptake rate is certainly the maximal value $u_{\max}$. When the insulin concentration is between $I_{\text{off}}$ and $I_{\text{on}}$, then the rate adheres to the current value, which can be either 0 or $u_{\max}$.

The simulation requires the assignment of the parameter $u_{\max}$. Notice that $N \cdot u_{\max}$ is the rate of glucose uptake when *all* the cells have been activated, which corresponds to $U_{\max} = V_{\max} - V_0 = 0.114\ \text{min}^{-1}$ in the insulin clamp data:

$$N \cdot u_{\max} = U_{\max}.$$

Because $N = 10^5$ is used, one has $u_{\max} = 1.14 \times 10^{-6}$. In fact, one can use other $N$ values as long as they are sufficiently large and as long as $u_{\max} = U_{\max}/N$ is adjusted. According to my trials, the simulations are almost the same as long as $N > 10^3$.

The simulation goes as follows. With the initial values $t = 0$, $G(0) = G_0$, and $I(0) = I_0$, equations 1 and 2 are integrated. In every time step, the body's rate of glucose uptake is determined by equations S.8 and S.9, which take into account every cell's contribution. The simulation stops when $t = T$ is reached. The black curve in figure 4C is the simulated $G(t)$ when $\Delta I = 5$ $\mu$U/ml is used. The red curve in figure 4C is the simulated $G(t)$ when $\Delta I = 10$ $\mu$U/ml is used.

For both cases, the glucose level stabilized to a value below the baseline $G_0$, indicative of potential hypoglycemia. The larger $\Delta I$, the larger the undershoot, and more severe the hypoglycemia. To determine the conclusion's sensitivity to the parameters, the simulation is repeated $10^4$ times for the case $\Delta I = 5$. Each simulation is based on a new set of parameter values. Figure S.2C shows the histogram of the quantity $G(T)/G_0 - 1$, which is strictly to the left of the longitudinal axis, indicating that the quantity is always negative, i.e., the occurence of reactive hypoglycemia is $10^4/10^4$. The same phenomenon is observed for the case $\Delta I = 10$ (figure S.2D). For the case $\Delta I = 0$, it is expected that the histogram (figure S.2B) should be similar to that under the graded response view (figure S.2A), which is indeed the case. The key observation is that hysteresis is strictly correlated with reactive hypoglycemia, suggesting that the adjustable threshold hypothesis is correct.

## Reference


[App1] Topp, B., Promislow, K., deVries, G., Miura, R. M. & Finegood, D. T. 2000 A model of beta-cell mass, insulin, and glucose kinetics: pathways to diabetes. *J Theor Biol* **206**, 605–619.

[App2] Wang, G. 2012 Optimal homeostasis necessitates bistable control. *J R Soc Interface* **9**, 2723–2734.

[App3] Bonadonna, R. C., Groop, L., Kraemer, N., Ferrannini, E., Del Prato, S. & DeFronzo, R. A. 1990 Obesity and insulin resistance in humans: a dose-response study. *Metabolism* **39**, 452–459.

[App4] Baron, A. D. 1999 Vascular reactivity. *Am J Cardiol* **84**, 25J–27J.

[App5] Fox, S. 2007 *Human Physiology* 10th edn. Dubuque, IA: McGraw-Hill Science/Engineering/Math

[App6] Porte, D., Sherwin, R. S. & Baron, A. 2002 *Ellenberg and Rifkin's diabetes mellitus.* 6th edn. New York, NY: McGraw-Hill Professional

[App7] Toffolo, G., Bergman, R. N., Finegood, D. T., Bowden, C. R. & Cobelli, C. 1980 Quantitative estimation of beta cell sensitivity to glucose in the intact organism: a minimal model of insulin kinetics in the dog. *Diabetes* **29**, 979–990.

[App8] Bergman, R. N., , Phillips, L. S. & Cobelli, C. 1981 Physiologic evaluation of factors controlling glucose tolerance in man: measurement of insulin sensitivity and beta-cell glucose sensitivity from the response to intravenous glucose. *The Journal of clinical investigation* **68**, 1456–1467.

[App9] Malaisse, W., Malaisse-Lagae, F. & Wright, P. H. 1967 A new method for the measurement in vitro of pancreatic insulin secretion. *Endocrinology* **80**, 99–108.

[App10] Polonsky, K. S., Given, B. D. & Van Cauter, E. 1988 Twenty-four-hour profiles and pulsatile patterns of insulin secretion in normal and obese subjects. *J Clin Invest* **81**, 442–448.

[App11] Sturis, J., Polonsky, K. S., Mosekilde, E. & Van Cauter, E. 1991 Computer model for mechanisms underlying ultradian oscillations of insulin and glucose. *Am J Physiol* **260**, 801–809.